Analytical Investigation of Slab Bridges with Integral Wall Abutments

H. J. DAGHER, M. ELGAALY, AND J. KANKAM

The design of a single-span bridge with integral wall abutments is simple when the bridge has no skew. For skewed bridges, the design is complicated by higher shears and moments that develop near the obtuse angle. The finite element method can be used to compute these moments and shears; however, it is time consuming for everyday design unless specialized pre- and postprocessors are available. A linear elastic finite element analysis was used to investigate the effects of dead loads, AASHTO live loads, and earth pressures on 20 different bridges with spans ranging from 15 to 60 ft and skew angles varying from 0 to 60 degrees. The results of the study have been used to produce charts that are adequate for design purposes. These charts relate the moments, shears, and deflections in a skew bridge to those in a 1-ft-wide plane frame taken along the longitudinal center line of the skew bridge. Work to refine and verify the results obtained to date through laboratory model testing and nonlinear finite element analysis is ongoing.

The slab bridges considered in this study are rigidly connected to supporting wall abutments. A recent nationwide survey conducted by the authors indicated that 22 states had a total of 11,500 bridges of this type, both skew and straight, either already existing or projected for the future (*1*). Two major reasons for building such bridges are the reduction of positive moments and the elimination of bridge deck expansion joints, thus reducing construction and maintenance costs. Conventional bridge bearing devices often become ineffective and are susceptible to deterioration from roadway runoff through open or leaking deck joints.

Many investigations have been conducted on the behavior of skew slabs under load. However, most of this work relates to skew slabs that are supported on columns, beams, or on nonintegral supports.

Bakht (*2*) proposed that skew slab-on-girder bridges having $(s \tan(\alpha)/L) < 0.05$ could be analyzed as equivalent right bridges, where s, L, and α are the girder spacing, bridge span, and skew angle, respectively. Cheung et al. (*3*) presented a general finite element program that could be used to evaluate bending moments and support reactions in complex modern bridges of any shape. Clark (*4*) suggested a method of preventing punching shear when a concentrated load is near a free edge of a reinforced-concrete slab.

Cope et al. (*5–13*) outlined a nonlinear method for analyzing slab bridges; the method was considered to be expensive and was therefore recommended only for assessment of more approximate design methods or for analysis of complicated one-off structures. They also observed from laboratory tests on five 1:5-scale, reinforced-concrete, column-supported skew slabs that shear failure was always initiated in the free-edge zone and that increasing skew angle considerably decreased the shear capacity of a slab. The presence of vertical bonded reinforcement at the free edge produced considerable enhancement to the overall shear capacity of a slab. Also, slabs with the main reinforcement parallel to the free edges were found to possess better load distribution properties than those with the main reinforcement perpendicular to supports and were therefore less likely to undergo punching shear failure when subjected to heavy concentrated loading. They also found that predicted shear forces from thick- and thin-plate analyses of slabs were broadly in agreement except in the edge zones (with widths of about two slab thicknesses for a 45-degree skew slab) were thick-plate theories indicated much higher shear stresses. They recommended that when the design of bridge slabs is based on the results of thin-plate theory, reactions provide a better guide to the distribution of shear forces in obtuse corner regions than do values of shear forces predicted from derivatives of moments.

Mahmoudzadeh et al. (*14*) conducted parametric studies of 54 reinforced-concrete, multispan, slab bridges with a finite element program called GENDEK-5 to assess the effects of skew on support reactions and internal bending moments. They observed that

1. Maximum positive and negative slab moments were governed by AASHTO alternate loading and HS20 truck loads, respectively, except that the alternate loading governed both moments at 60-degree skews;
2. Longitudinal bending moments were significantly reduced with increasing skew angle;
3. The alternate loading was the controlling factor for abutment total reactions;

Rusch and Hergenroder (*15*) published 174 contour charts of influence surfaces for bending moments and torsional moments in skew slabs. The charts were based on tests on models and cover skew angles of 30, 45, and 60 degrees.

Greimann et al. (*16*) summarized the findings of a survey of the highway departments of all 50 states to obtain information on the design and performance of skewed bridges with integral abutments. They concluded that there was a lack of theoretical and experimental research in this area, with the result that most states designed integral abutments on skewed bridges on the basis of empirical experience without adequate theoretical analysis.

Considerable research work has been conducted on the finite element analysis of reinforced concrete (*17,18*). In ad-

Civil Engineering Department, Boardman Hall, University of Maine, Orono, Maine 04469.

dition, many methods are available for the design and analysis of reinforced-concrete slabs. These methods include elastic theory, limit analysis theory, and modifications of the elastic and limit analysis theories as in the American Concrete Institute code. The design procedure is based on work by Wood (*19*) and Hillerborg (*20*). Considerable information on the behavior of reinforced-concrete slabs may be found in textbooks solely dedicated to RC slabs, such as those by Wood (*21*), Park and Gamble (*22*), and Cope and Clark (*23*).

LINEAR AND NONLINEAR ANALYSIS

Typically, design moments and shears in reinforced-concrete structures are obtained by conducting a linear elastic analysis of the structure using factored loads. The resulting moments and shears are then compared with the nominal ultimate capacity of a member.

Although this practice does not predict the actual moment and shear distributions at the limit state, it leads to conservative designs. This effect is because reinforced-concrete structures normally have enough ductility so that some redistribution of moments and shears is possible if the ultimate capacity is reached at one point. This has been recognized by the American Concrete Institute's building code, which has provisions for redistribution of moments at the supports of continuous flexural members.

The ability of reinforced concrete to redistribute moments is used in yield line analysis of slabs, which is commonly used for slab design in Scandinavian countries. When a portion of a slab reaches its ultimate capacity, the reinforcement will yield, and this portion of the slab will act as a plastic hinge that will hold a constant moment. When additional load is applied on the slab, the plastic hinge rotates and additional moment is transferred to adjacent sections that have not yet yielded.

The results presented are based on a linear elastic analysis using a University of Maine mainframe version of the SAP finite element program (*24*). The recommendations given are therefore conservative, and are being refined using nonlinear analysis and laboratory testing.

OBJECTIVE OF THIS STUDY

Integral skewed slab bridges are characterized by high moments and shears in the vicinity of the obtuse corners. This effect is shown in Figure 1 by the distribution of shear in the slab near the wall for a bridge with a 70-ft span and a 20-degree skew angle, subjected to self-weight. (The shear forces near the obtuse corners do not vanish because they are calculated using the membrane stresses at the center of the corner wall element adjacent to the slab.) Cracking near the obtuse corner of an integral skew slab bridge with these dimensions has been observed recently in Maine (*1*). Figure 2 shows the magnitudes of design moments at the obtuse and acute corners in an 84-ft-span bridge with a skew angle of 45 degrees. The irregularity of the curves in Figure 2 results from the definition of the design moments, which are different from the bending moments obtained directly from a finite element analysis. As described later, the design moments are obtained by combining the flexural and torsional moments from a finite element analysis.

The magnitude of flexural and shearing stresses in these bridges can be obtained using finite element analysis. However, the finite element analysis is time consuming for everyday design. There is therefore a need for simplified methods of determining design moments and shears. The objective of this study was to produce such design aids.

FINITE ELEMENT MODELING

The finite element models of the structure are composed of the following elements, available in the SAP Program (*24*):

1. Thin-plate elements with four nodes per element and five degrees of freedom per node were used in the walls and

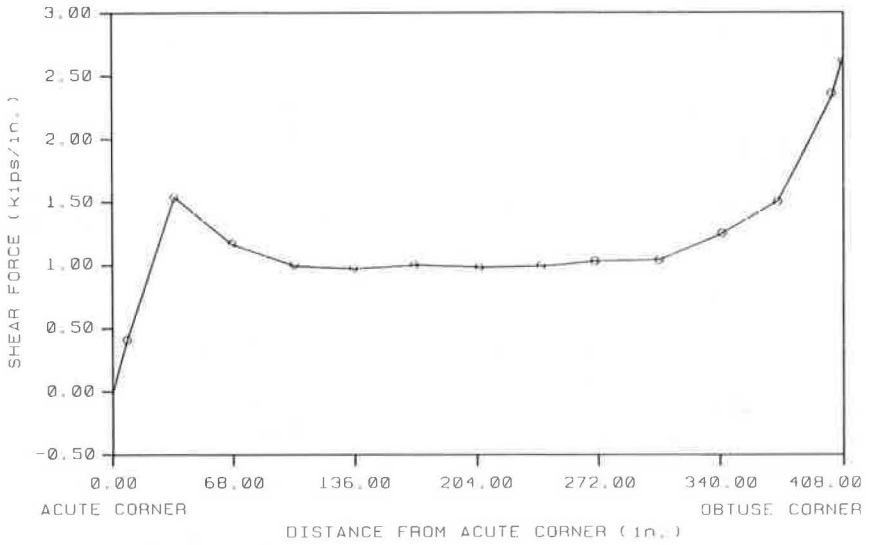

FIGURE 1 Typical shear force distribution in a skew slab at a support caused by self-weight.

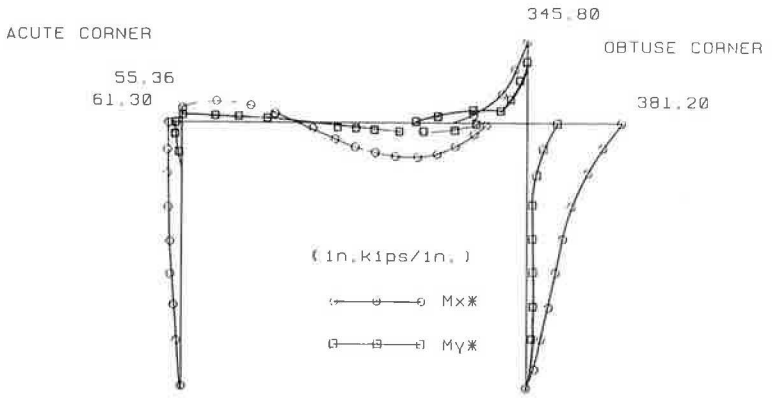

FIGURE 2 Typical distribution of design moments near the free edge of a skewed-slab bridge caused by self-weight.

skew slab. They were restrained against in-plane rotation (drilling) when the elements intersecting at the node were in the same plane.

2. Boundary elements were used to restrain the drilling degrees of freedom in plate elements when these were not in the direction of a global coordinate axis. Boundary elements were also used to obtain the reactive moments and forces at the base of the walls.

At the strength limit state, the moment of inertia of the walls was taken to be that of the gross cross section; the value for the slab was taken as half that of the gross cross section of the slab. This procedure reflects common design practice and is based on the assumption that flexural cracking of the slab requires the use of the cracked moment of inertia, whereas the walls are subjected to compressive dead and live loads that will reduce cracking. These assumptions are in line with the ACI318-89 (*25*), Section R.8.6.1.

An example of a finite element mesh used for the analysis is shown in Figure 3. A graded, finer mesh was used near the edges of the slab to better depict the high rate of change of moments and shears at these locations.

PREPROCESSOR

A special preprocessor was developed for rigid-frame skew slab bridgers that were to be analyzed with the SAP Finite Element Program (*1*). With the preprocessor, the user interactively specifies the overall dimensions, material properties, and loading conditions of the bridge. The preprocessor generates the numbers and coordinates of the nodes of the structure, the numbers and connectivities of the plate elements, the properties of the boundary elements, and other necessary data in the format required by SAP.

The preprocessor also generates AASHTO loadings automatically. For the AASHTO truck loadings for example, HS25 trucks are automatically moved across the bridge and the resulting nodal loads are automatically calculated.

CONVERGENCE STUDIES

Convergence studies were carried out using three models with 325, 665, and 1,000 plate elements.

For the structure shown in Figure 4, maximum vertical displacements caused by the self-weight of the structure (at point *P*), as well as maximum design moments (at point *E*), are plotted in Figure 5 for the three different models. Values for the models with 325 and 665 plate elements are expressed as percentages of corresponding values for the model with 1,000 elements.

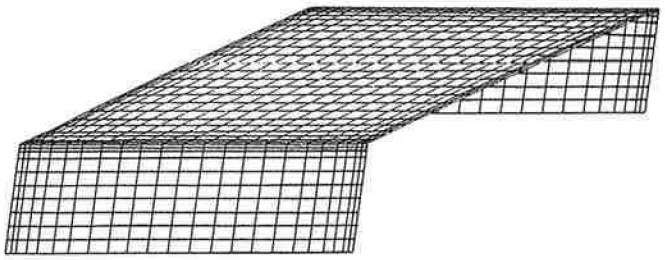

FIGURE 3 Typical finite element mesh of 1,000 elements used for rigid-frame skewed-slab bridge.

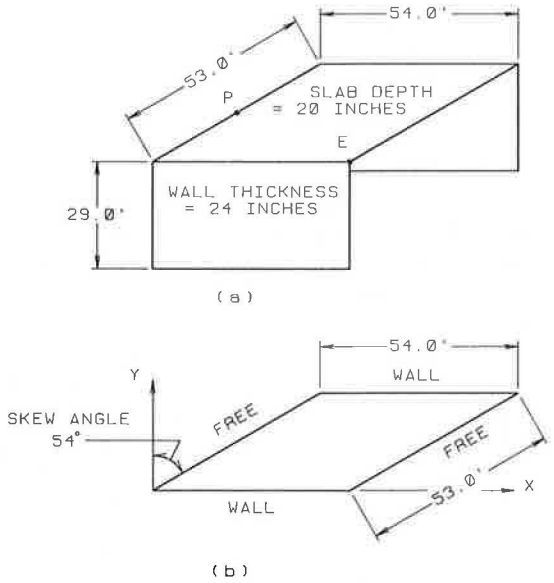

FIGURE 4 Structure used in convergence studies: (a) the whole frame, and (b) top view of slab.

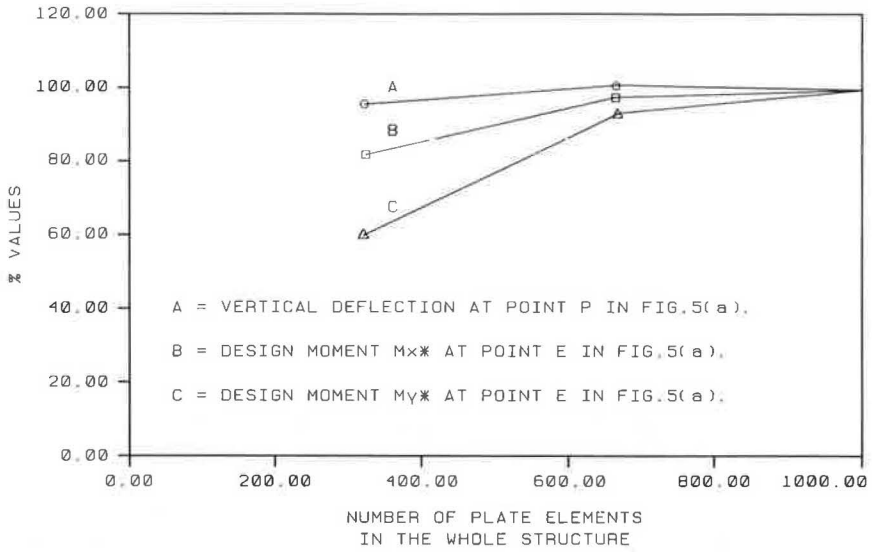

FIGURE 5 Convergence studies.

Increasing the number of elements from 325 to 665 results in an improvement of 16 percent (for Mx*) and 36 percent (for My*) in the moments and 5 percent in the displacements. An improvement of less than 10 percent on the moments, and less than 4 percent in the displacements is achieved by refining the model from 665 to 1,000 elements. The 1,000-element model was adopted for use in the parametric studies.

POSTPROCESSOR

A postprocessor was developed to convert the results of the finite element analysis into design moments, to plot moment envelopes for any longitudinal or transverse section, to plot shear envelope for the slab at the supports, and to record the maximum vertical displacement in the slab.

PARAMETRIC STUDY

In the parametric study, 20 different bridges were analyzed for 15 loading conditions each. The finite element analyses were significantly expedited by using the specialized pre- and postprocessors. In fact, routine analysis and design of skew slab bridges can be efficiently carried out on a personal computer should the appropriate finite element software and the specialized pre- and postprocessors be available. If this is the case, the design method proposed may serve for preliminary design.

Using the preprocessor, 2 min were required to prepare the SAP data file for each analysis. The actual time taken by the SAP program for each 1,000-element analysis was fewer than 200 sec on the University of Maine's IBM 3090 Model 200I Computer. However, because of time sharing with other jobs, the total time taken to get the results of the analysis was about 9 min.

For each analysis, a number of equilibrium checks were conducted, such as comparing the reactive forces at the base of the walls with the sum of the applied loads. The results of the parametric studies have been embodied in the design curves that are described elsewhere.

Geometries of Bridges

Based partly on AASHTO requirements for minimum lane width (*26*), ACI 343R-88 requirements for minimum depth of bridge slabs (*27*), and results of the nationwide survey, the following ranges of parameters were used in the parametric studies, which were expedited with the pre- and postprocessors:

- Skew angles 0, 15, 30, 45, and 60 degrees;
- Width at supports 30, 31, 35, 43, and 60 ft;
- Normal span 15, 30, 45, and 60 ft;
- Slab thickness 15, 18, 26, and 36 in.;
- Wall thickness 18, 21, 30, and 40 in.; and
- Wall height 20 ft.

Each value of the width of support listed previously corresponds to one skew angle only, so that a two-lane bridge with a 30-ft transverse width is always obtained. The edge beam had a width of 22 in. and a height of 36 in. above the slab. However, it was conservatively judged to be nonstructural, and its weight was applied as a line load. This decision was based on the fact that, in practice, the edge beam is often cast only after the slab has been cast and cured for some time and the supporting formwork has been removed.

Loading Conditions

The loading conditions used for the parametric studies were composed of the following (Figure 6):

1. Self-weight including a 825-lb/ft edge beam;
2. AASHTO HS25 lane loads;
3. AASHTO HS25 truck loads;

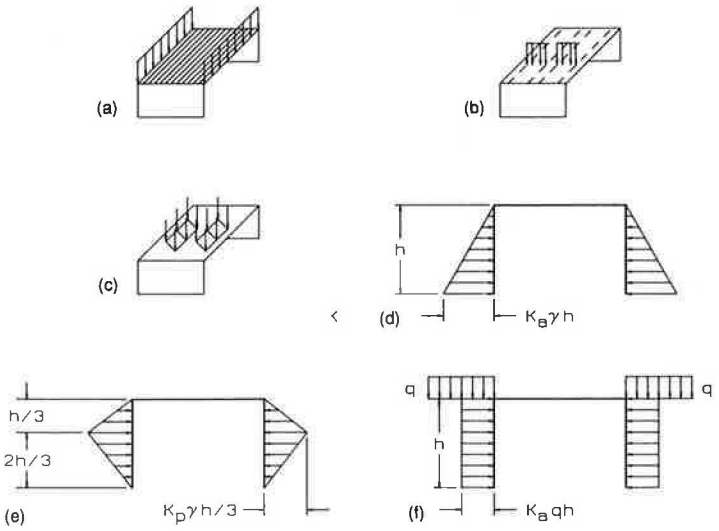

FIGURE 6 Loading conditions used in parametric studies: (a) self-weight including 825-lb/ft edge beam, (b) AASHTO HS25 lane loads for typical two lanes, (c) AASHTO HS25 truck loads for typical two lanes, (d) active earth pressure, (e) passive earth pressure, and (f) surcharge.

4. A triangular earth pressure distribution with a generic maximum value of 100 lb/ft² at the base of the walls and a value of zero at the top of the walls;

5. A passive earth pressure with a generic value of 100 lb/ft² at a depth of one-third the wall height, which linearly varies to zero at the top and bottom of the walls. This distribution is based on results of field measurements reported by Elgaaly et al. (*28*);

6. Uniform earth pressure with a generic value of 100 lb/ft² to represent the effect of surcharge; and

7. A uniform load of 100 lb/ft² on the slab (not shown in Figure 6).

For the AASHTO truck loads, one HS25 truck was used per design lane. The trucks were placed on the bridge at 10 successive locations, starting from one wall and extending to the other. For the lane loadings, the line loads were placed at the center of the slab and then near the wall. Results obtained from these analyses were used to plot an envelope of maximum live load moments for the bridge. For the range of spans considered, the AASHTO truck load condition controls the live load stresses.

For each combination of bridge and type of load, a corresponding two-dimensional frame analysis was carried out, the frame chosen being a 1-ft-wide strip taken along the longitudinal center line of the bridge. Live load analysis for the frame was based on Paragraph 3.24.3.2 of the AASHTO Standard Specifications (*26*).

Results of the parametric studies for 20 different bridges and their corresponding frames were used to produce the design curves whose description follows.

DESIGN CURVES

The design curves allow conversion of the results from a plane frame analysis to values that apply for a skew slab bridge with integral slab abutments. The frame analysis must be conducted following the guidelines in AASHTO, Paragraph 3.24.3.2 (*26*), using a 1-ft-wide longitudinal strip taken along the skew span of the bridge. The design curves allow the calculation of moments, shears, and deflections at selected points in the skew slab bridge (see Figure 7).

Range of Design Curves

The design curves were produced for skew angles ranging from 0 to 60 degrees, and for aspect ratios varying from 0.5 to 2.0. The skew angle is defined as the amount by which the angle at the acute corner of the plan view of the slab is less than 90 degrees. The aspect ratio is defined as the ratio

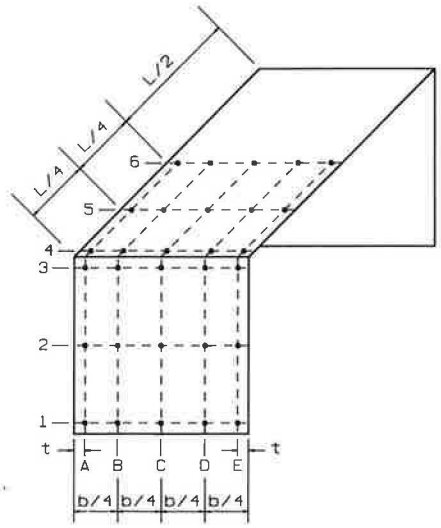

FIGURE 7 Reference points for design curves.

L/W, where L is the skew span of the bridge and W is the width of the slab along a support. The wall thicknesses used in the studies were always 3 or 4 in. greater than the corresponding slab thicknesses.

Initially, the parametric studies included analyses with the base of the wall both fixed and free. Figure 8 shows typical details for pinned and fixed wall bases. Results indicated that the restraint condition at the base of the wall does not, for most practical purposes, influence the distribution of stresses in the slab. The two-dimensional rigid frame analysis, which still needs to be conducted before the proposed charts are used, can take into account any restraint condition at the base of the wall. The design charts will simply distribute the moments thus obtained across the width of the bridge.

Assumed Steel Orientation in Design Curves

The design curves assume that the steel reinforcement will be placed parallel and perpendicular to the center line of the bridge (Figure 9). The 90-degree orientation between the longitudinal and transverse reinforcements results in the least amount of steel required. However, it will result in slightly higher fabrication costs because the transverse bars will not all be of the same length.

Design Moments for Flexure and Torsion

Figure 10 shows the directions of the coordinate axes and notation for moments. The bending moments Mx and My and the torsional moments Mxy produced by the finite element analysis are converted into the design moments Mx* and My* according to the following equations (*19*):

$$Mx^* = Mx \pm |Mxy|$$
$$My^* = My \pm |Mxy|$$

where

Mx* = design moment for reinforcement in the slab parallel to the skew span (Figure 9) and for vertical reinforcement in the wall, and

My* = design moment for reinforcement in the slab perpendicular to the skew span (Figure 9) and for horizontal reinforcement in the wall.

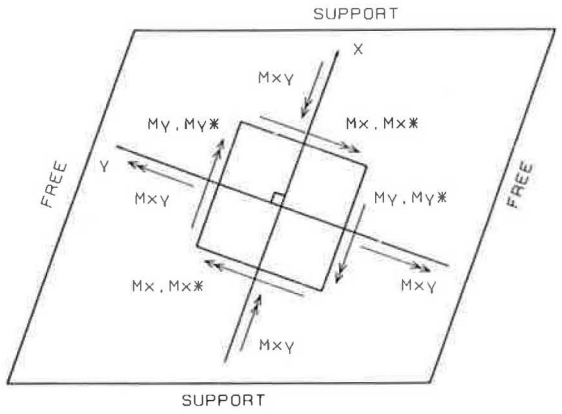

FIGURE 10 Plan view of the slab showing directions of coordinate axes and notation for positive moments.

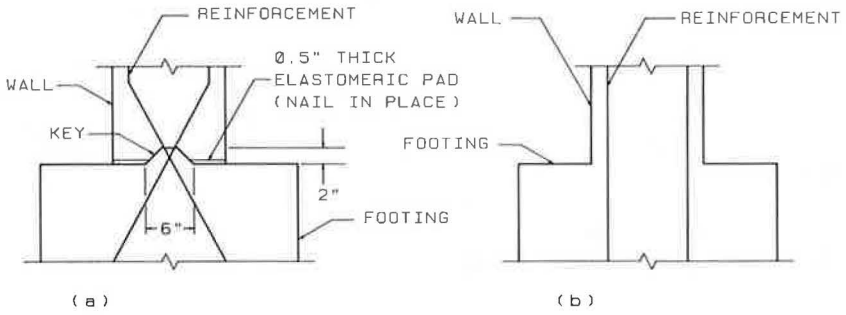

FIGURE 8 Typical details at the bottom of the abutment wall: (a) pinned base, and (b) fixed base.

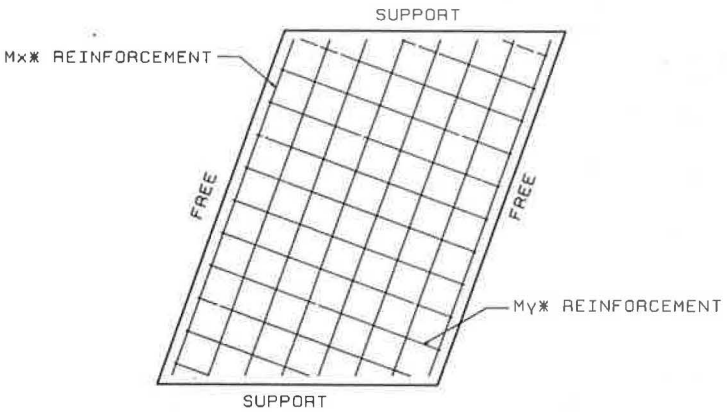

FIGURE 9 Design moments on plan view of slab.

The term "design moments" refers to equivalent bending moments for which reinforcement can be specified to account for both the flexural and torsional moments obtained from the finite element analysis. This concept, which is widely used in Great Britain and Europe, was originally developed by Hillerborg (*20*) and further extended by Wood (*19*); it is being further investigated.

Because of the assumptions in thin-plate theory that form the basis for the finite element analysis and the inaccuracies related to mesh size, certain limitations apply to the interpretation of the twisting moments, which are high and which do not go to zero at the free edges as they are supposed to do according to Kirchhoff boundary conditions. The design moments Mx* and My*, which include these twisting moments, consequently become artificially high near the free edges of the slab, and have therefore been discarded in this region.

In the design curves, moments near the obtuse or acute corners have been taken at a distance t from the free edge of the slab (t = slab thickness). For example, in Figure 11, the ratio Mx*/Mxp is given at point *E*4, which is at distance t from the free edge of the slab. For zero skew and an aspect ratio of 0.5, Figure 11 yields Mx*/Mxp = 1.8 for self-weight plus edge beam weight. If the edge beam did not exist, this ratio would have been equal to one for zero skew.

The design curves allow the calculation of design moments at 30 selected locations covering one-half of the bridge, as shown in Figure 7. For example, moments may be computed at point *A*2, located at the intersection of Longitudinal Line *A* and Transverse Line 2 shown in Figure 7. Line *A* is a longitudinal line parallel to the center line of the bridge and located at a distance equal to the slab thickness t from the free edge. For self-weight and AASHTO live load, Line 2 goes through the midheight of the wall; for each pressure, it goes through the point of maximum positive moment in the wall.

For a given point and type of load, the design curves yield the ratios Mx*/Mxp and My*/Mxp of the design moments in the slab to those in the corresponding plane frame for different aspect ratios and skew angles, where Mxp is the bending moment at the corresponding point in the two-dimensional frame. For points *A*2, *B*2, *C*2, *D*2, and *E*2, for instance, the corresponding point in the two-dimensional frame taken along the longitudinal center line would be *C*2; whereas for points *A*4, *B*4, *C*4, *D*4 and *E*4, the corresponding point would be *C*4.

Figures 11 and 12 show typical moment design curves for point *E*4 under self-weight plus edge beam. A complete set of design curves was provided by Dagher et al. (*1*).

Design for Shear

Figures 13 and 14 show typical shear design curves for point *E*4 under self-weight plus edge beam weight and for point *D*4 under AASHTO live loads, respectively. The curves yield the ratios Vs/Vp for different aspect ratios and skew angles, where Vs is the shearing force (force per unit width) at the reference point in the skew slab; and Vp is the shearing force at the corresponding point in the two-dimensional frame.

A typical curve of Vs/Vp is shown in Figure 15. As stated earlier, the full design guide (*1*) does not yield moment and shear ratios within distance t from the free edge, because of concerns about the accuracy of the model in these regions. For self-weight plus edge beam, Figure 14 shows design curves for the maximum values of Vs/Vp that occur between point *E*4 and the free edge near the obtuse corner. Whether these should be used in design rather than the values at point *E*4 is a matter that requires further research.

Maximum Vertical Displacement

Figures 16 and 17 show typical displacement design curves. The curves give the ratios Ds/Dp for different aspect ratios and skew angles, where Ds is the maximum vertical displacement in the slab and Dp is the maximum vertical displacement in the corresponding two-dimensional frame.

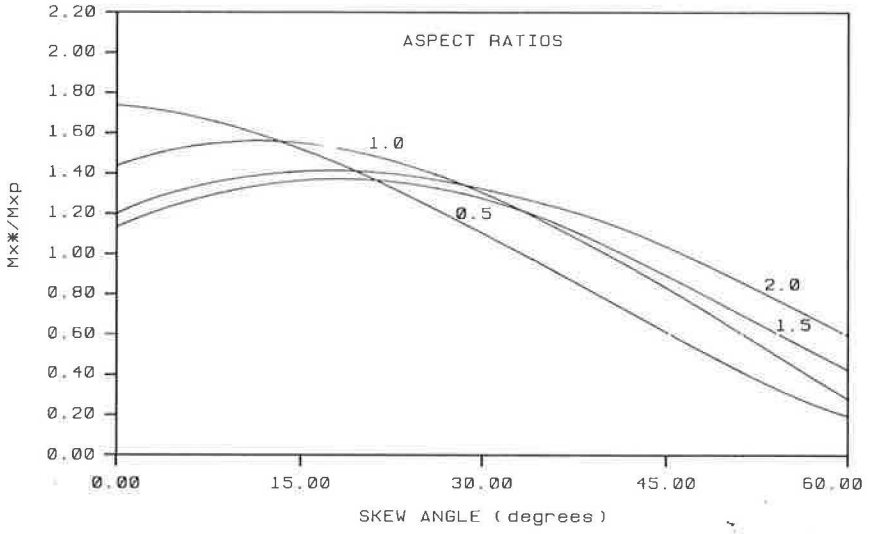

FIGURE 11 Pinned-base bridges under self-weight plus edge beam weight—curves for Mx*/Mxp at Point *E*4.

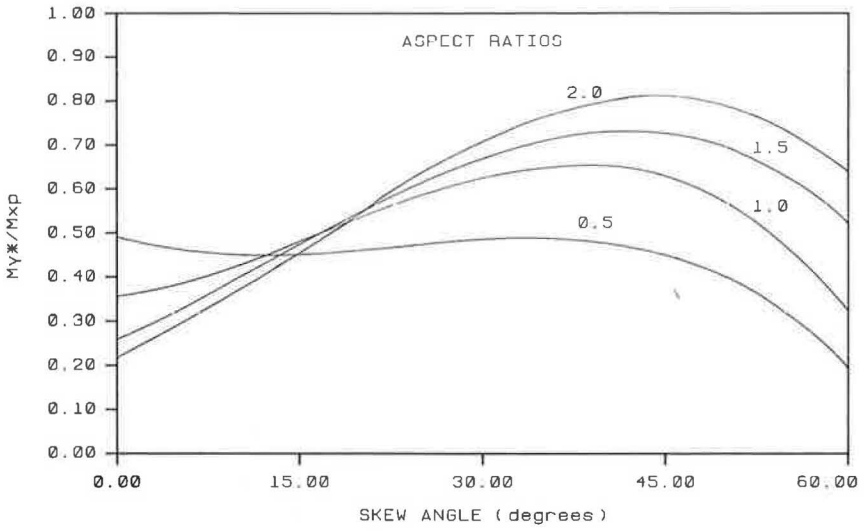

FIGURE 12 Pinned-base bridges under self-weight plus edge beam weight—curves for My*/Mxp for Point *E*4.

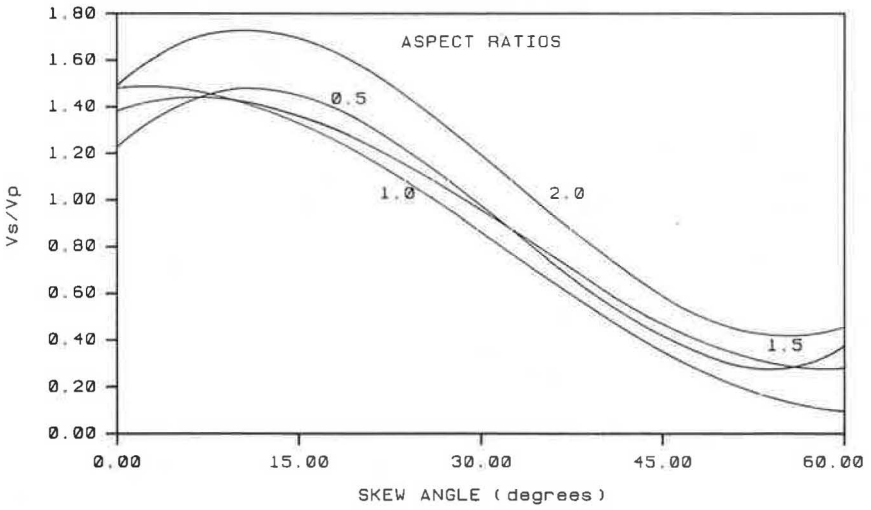

FIGURE 13 Pinned-base bridges under self-weight plus edge beam weight—curves for Vs/Vp at Point *E*4.

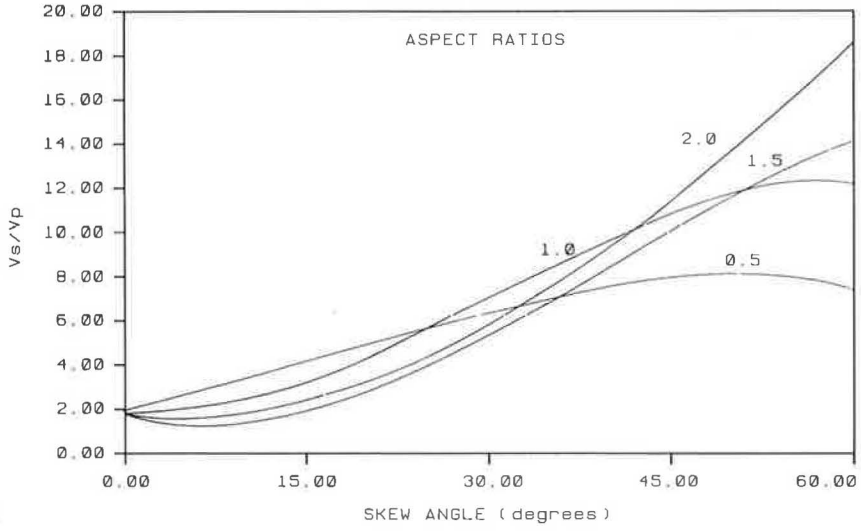

FIGURE 14 Pinned-base bridges under self-weight plus edge beam weight—curves for Vs/Vp between Point *E*4 and the free edge.

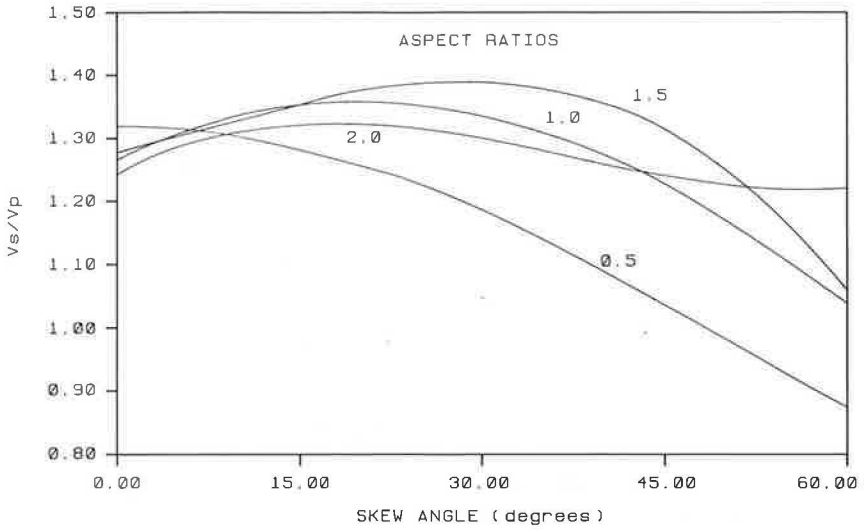

FIGURE 15 Pinned-base bridges under live load—curves for Vs/Vp at Point *D*4.

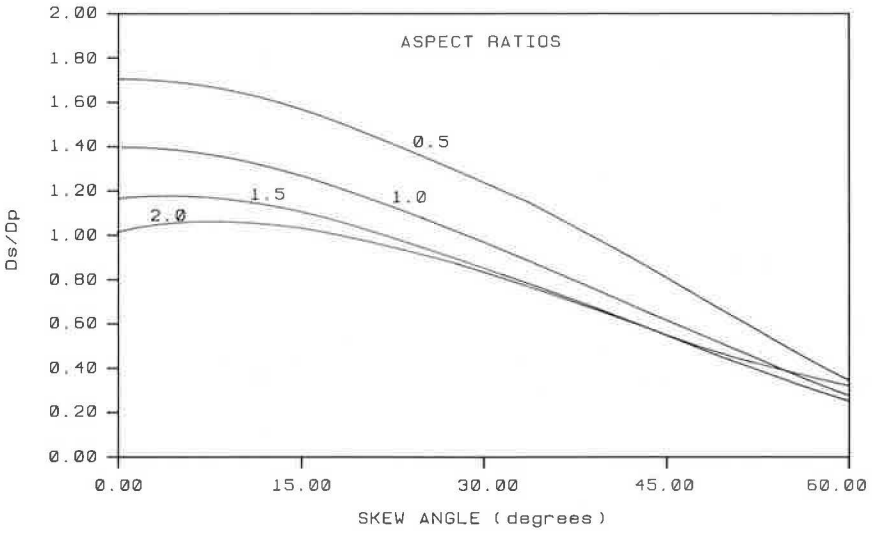

FIGURE 16 Pinned-base bridges under self-weight plus edge beam weight—curves for Ds/Dp.

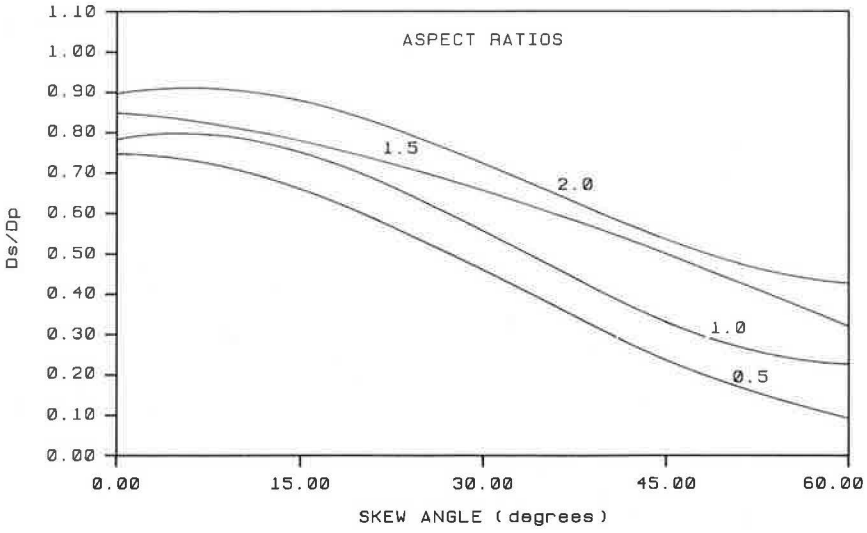

FIGURE 17 Pinned-base bridges under live load—curves for Ds/Dp.

EXAMPLE ON USE OF DESIGN CURVES

The following example illustrates the use of the design curves. A bridge may begin with the following properties:

- Skew span = 73.6 ft,
- Width along support = 34 ft, and
- Skew angle = 20 degrees.

It is then required to find the design moments at point *E*4 in the slab caused by self-weight and the weight of the edge beam.

The solution consists of the following steps:

- Step 1. Extract the equivalent 1-ft-wide two-dimensional frame for the bridge following the guidelines in AASHTO, Paragraph 3.24.3.2 (*26*).
- Step 2. Conduct a two-dimensional frame analysis for the load under consideration. For the given problem, this procedure results in a negative moment (Mxp) of 146.83 ft-kips/ft width in the slab near the wall.
- Step 3. Using a skew angle of 20 degrees and an aspect ratio of 73.6/34 = 2.2, obtain the design ratios from the uniformly distributed load design curves for point *E*4; i.e., Mx*/Mxp = 1.38 and My*/Mxp = 0.552.
- Step 4. Multiply the moments obtained in Step 2 by the design ratios in Step 3 to obtain the design moments:

Mx* = 1.38 × 146.83 = 202.9 ft-kips/ft
My* = 0.552 × 146.83 = 81.05 ft-kips/ft

In order to review the accuracy of the design curves, the predicted values of Mx* and My* were compared with the corresponding values obtained directly from a three-dimensional finite element analysis:

Mx* (from finite element analysis) = 215.1 ft-kips/ft
My* (from finite element analysis) = 81.89 ft-kips/ft

The discrepancy between predicted and computed values of Mx* is only 5.7 percent, whereas the discrepancy for My* is only 1.0 percent.

CONCLUSIONS

1. Integral reinforced-concrete skew slab bridges have relatively high shears and moments near the obtuse corner of the slab.
2. The literature reviewed did not reveal any previous theoretical or experimental research directly related to this problem.
3. The current design practice of providing for the transverse reinforcement with temperature and shrinkage reinforcement (AASHTO, Paragraph 8.20) or distribution reinforcement (AASHTO, Paragraph 3.24.10.2) may be inadequate.
4. A plane frame analysis of a skew slab bridge conducted following the guidelines in AASHTO, Paragraph 3.24.3.2, and using the skew span of the bridge can underpredict values of shear and moment near the obtuse corners. The magnitude of the resulting error depends on the skew angle and the aspect ratio of the bridge.
5. The degree of fixity at the base of the wall does not, for most practical situations, affect the distribution of shear and moments in the slab.
6. The research reported is still in progress and the published results are preliminary, based on linear finite element analyses. Laboratory testing of scale models and nonlinear analyses are underway to verify and refine the results presented herein.

ACKNOWLEDGMENTS

This investigation was sponsored by the Maine Department of Transportation. The assistance and helpful comments of Stephen Abott, Warren Foster, Brian Pickard, Leon Taylor, and John Buxton of the Maine Department of Transportation are greatly appreciated.

REFERENCES

1. H. J. Dagher, M. Elgaaly, J. Kankam, and L. Comstock. *Skew Slab Bridges with Integral Slab Abutments*: Vols. 1–6. Civil Engineering Department, University of Maine, Orono, Feb. 1991.
2. B. Bakht. Analysis of Some Skew Bridges as Right Bridges. *Journal of Structural Engineering, ASCE*, Vol. 114, No. 10, 1988, pp. 2307–2322.
3. Y. K. Cheung, I. P. King, and O. C. Zienkiewicz. Slab Bridges with Arbitrary Shape and Support Conditions: A General Method of Analysis Based on Finite Elements. *Proc., Institute of Civil Engineers*, Vol. 40, 1968, pp. 9–36.
4. L. A. Clark. Punching Shear Near the Free Edges of Slabs. *Concrete*, Aug. 1984, pp. 15–17.
5. R. J. Cope and P. V. Rao. Non-Linear Finite Element Analysis of Concrete Slab Structures. In *Proc., Institute of Civil Engineers*, Part 2, Marshalltown, South Africa, 1977, pp. 159–179.
6. R. J. Cope, P. V. Rao, and K. R. Edwards. Non-Linear Finite Element Analysis Techniques for Concrete Slabs. In *Proc., International Conference on Numerical Methods for Non-Linear Problems*, Swansea, Wales, 1980, pp. 445–456.
7. R. J. Cope and P. V. Rao. A Two-Stage Procedure for the Non-Linear Analysis of Slab Bridges. In *Proc., Institute of Civil Engineers*, Part 2, Vol. 75, Marshalltown, South Africa, Dec. 1983, pp. 671–688.
8. R. J. Cope and P. V. Rao. Moment Distribution in Skewed Slab Bridges. In *Proc., Institute of Civil Engineers*, Part 2, Vol. 75, Marshalltown, South Africa, Sept. 1983, pp. 419–451.
9. R. J. Cope and P. V. Rao. Shear Force in Edge Zones of Concrete Slabs. *The Structural Engineer*, Vol. 62A, No. 3, Mar. 1984, pp. 87–92.
10. R. J. Cope. Material Modelling of Real Reinforced Concrete Slabs. In *Proc., International Conference on Computer-Aided Analysis and Design of Structures*, Part I, Split, Yugoslavia, Sept. 1984, pp. 85–117.
11. R. J. Cope. Flexural Shear Failure of Reinforced Concrete Slab Bridges. In *Proc., Institute Civil Engineers*, Part 2, Vol. 79, Sept. 1985, pp. 559–583.
12. R. J. Cope and L. A. Clark. *Concrete Slabs: Analysis and Design*. Elsevier, London and New York, 1989.
13. R. J. Cope, P. V. Rao, and K. R. Edwards. *Shear in Skew Reinforced Concrete Slab Bridges*. Department of Civil Engineering, University of Liverpool, England, Oct. 1983.
14. M. Mahmoudzadeh, R. E. Davis, and F. M. Semans. *Modification of Slab Design Standards for Effects of Skew*. FHWA, U.S. Department of Transportation, 1984.
15. H. Rusch and A. Hergenroder. *Influence Surfaces of Moments in Skew Slabs*. Werner-Verlag, Dusseldorf, Germany, 1969.

16. L. F. Greimann, A. M. Wolde-Tinsae, and P. S. Yang. Skewed Bridges with Integral Abutments. In *Transportation Research Record 903*, TRB, National Research Council, Washington, D.C., 1983.
17. *Finite Element Analysis of Reinforced Concrete*. Task Committee on Finite Element Analysis of Reinforced Concrete Structures, ASCE, New York, 1982.
18. Finite Element Analysis of Reinforced Concrete Structures. Proc., Joint Seminar, Japan Society of the Promotion of Science and the National Science Foundation, C. Meyer and H. Okamura, eds., ASCE, New York, 1985, 685 pp.
19. R. H. Wood. The Reinforcement of Slabs in Accordance with a Predetermined Field of Moments. *Concrete*, Feb. 1968, pp. 69–76.
20. A. Hillerborg. Reinforcement of Slabs and Shells Designed According to the Theory of Elasticity. *Betong 1953*, pp. 101–109.
21. R. H. Wood. *Plastic Analysis and Design of Slab and Plates*. Thames and Hudson, London, 1961, 344 pp.
22. R. Park and W. L. Gamble. *Reinforced Concrete Slabs*. John Wiley, New York, 1980, 618 pp.
23. R. J. Cope and L. A. Clark. *Concrete Slabs: Analysis and Design*. Elsevier Applied Science, London and New York, 1984, 502 pp.
24. K. J. Bathe, E. L. Wilson, and F. E. Peterson. *SAP4: Structural Analysis Program for Static and Dynamic Response of Linear Systems*. University of California, Berkeley, 1964.
25. *Building Code Requirements for Reinforced Concrete*. ACI 318-89. American Concrete Institute, Detroit, Mich., 1989.
26. *Standard Specifications for Highway Bridges*, 13th ed. AASHTO, Washington, D.C., 1983.
27. *Analysis and Design of Reinforced Concrete Bridge Structures*. ACI 343R-88. American Concrete Institute, Detroit, Mich., 1988.
28. M. Elgaaly, T. Sandford, and C. Colby. *Monitoring the Forks Bridge to June 6, 1990*. Maine Department of Transportation, Augusta, Dec., 1990.

Publication of this paper sponsored by Committee on Concrete Bridges.